Controlled type-I–type-II transition in GaAs/AlAs/$Al_xGa_{1-x}As$ double-barrier quantum wells

B. Chastaingt
Centre de Recherche sur l'Hétéroépitaxie et ses Applications, Centre National de la Recherche Scientifique, rue B. Grégory, F-06560 Valbonne, France

M. Gurioli, P. Borri, and M. Colocci
Istituto Nazionale per la Fisica della Materia and Laboratorio Europeo di Spettroscopie Non Lineari, Dipartimento di Fisica, Largo E. Fermi 2, I-50125 Firenze, Italy

G. Neu, C. Deparis, and J. Massies
Centre de Recherche sur l'Hétéroépitaxie et ses Applications, Centre National de la Recherche Scientifique, rue B. Grégory, F-06560 Valbonne, France

J. Martinez-Pastor
Departament de Fisica Aplicada, Universitat de Valencia, E-46100 Burjassot, Spain
(Received 25 June 1996; revised manuscript received 11 September 1996)

We show that the insertion of extremely narrow AlAs layers in double-barrier GaAs/AlAs/$Al_xGa_{1-x}As$ quantum wells results in a variety of electronic configurations, thus providing a powerful tool for tailoring the electronic transitions in GaAs heterostructures. In particular, the transition from type-I to type-II recombination is shown to occur in correspondence with variations by a single monolayer in the thickness of the AlAs and/or GaAs layers. Drastic changes in the recombination lifetimes are correspondingly observed; at the same time, the photoluminescence efficiency is found to be almost independent of the type-I–type-II character of the transition. [S0163-1829(97)04904-7]

I. INTRODUCTION

Increasing attention has been devoted recently to type-II GaAs/$Al_xGa_{1-x}As$ heterostructures in which the ground level for the holes is a Γ state in the GaAs region, while the lowest level for the electrons is an X state in the $Al_xGa_{1-x}As$ region.[1–3] In this kind of heterostructure the radiative recombination turns out to be indirect both in k space and in real space and therefore dramatic changes of the optical properties are expected with respect to the more commonly studied type-I systems. So far most of the work on this subject has been performed in thin GaAs/AlAs quantum wells[4] (QW's) and superlattices (SL's);[5–7] in fact, in these structures, the confinement energy of the Γ conduction-band state increases when reducing the GaAs thickness, so that, below 35 Å, the ground electronic level of the structure is an X state in the AlAs layers.

A different approach used in order to achieve the type-I–type-II transition consists of applying a hydrostatic pressure.[8,9] Due to the opposite variations of the Γ and X band gaps with pressure, a crossover is eventually expected in all kinds of GaAs/$Al_xGa_{1-x}As$ heterostructures.

In this paper we show that a different kind of heterostructure, namely, double-barrier quantum wells (DBQW's), in which an ultrathin layer of AlAs is inserted between the $Al_xGa_{1-x}As$ and GaAs regions, provides a very favorable system for studying the type-I–type-II transition. In fact, with a proper choice of the growth parameters, a large variety of electronic configurations is allowed in these structures: the ground level can be a bound or an unbound state for both the holes and the electrons and even, in the latter case, a Γ or an X state. Indeed, as shown below, a detailed analysis of frequency and time-resolved photoluminescence (PL) spectra demonstrates the occurrence of the type-I–type-II transition. The dependence of the optical transition energies on the AlAs and GaAs thicknesses is in agreement with the predictions of a simple envelope function model, which confirms the occurrence of the type-I–type-II transition when the number of GaAs monolayers is reduced below a critical value. This transition is dramatically demonstrated by the time-resolved measurements where jumps in the decay times from 400 ps to 600 ns are observed when switching from type-I to type-II heterostructures, without major changes in the PL efficiency. From the experimental data we estimate the value of the Γ-X mixing potential to be of the order of 4 meV.

The paper is organized as follows. In Sec. II we develop a simple model for calculating the confinement energies for the Γ and X potential profiles. A phaselike diagram for the electronic configuration is presented, showing the possibility of type-II DBQW's with a proper choice of the structural parameters. Details of the samples investigated and the experimental apparatus used are reported in Sec. III. Section IV is devoted to the presentation of the experimental results and their discussion. Concluding remarks are given in Sec. V.

II. ELECTRONIC CONFIGURATION

In this section, we analyze the electronic properties of $Al_xGa_{1-x}As$/AlAs/GaAs DBQW's in the framework of the effective-mass approximation. In this kind of heterostructures one has to deal with both the Γ and X band-gap pro-

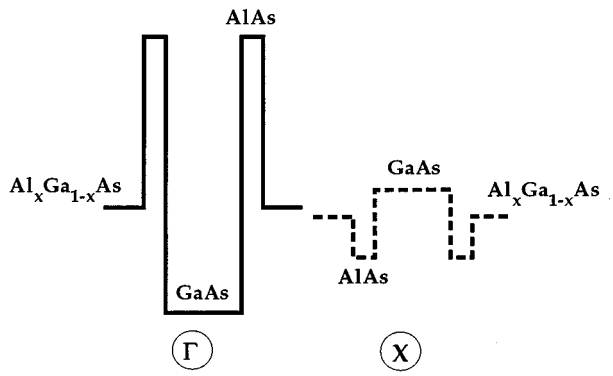

FIG. 1. Γ and *X* band-gap profiles.

files, which are depicted in Fig. 1. In fact, since the AlAs is an indirect semiconductor and given the band-offset ratio at the $Al_xGa_{1-x}As$/GaAs interface, DBQW's can support a bound state for both the *X* and Γ profiles under suitable values of the Al concentration and layer thicknesses. In order to solve the eigenvalue problem and to find the bound-state energies, we analyze the two potential schemes reported in Fig. 1 independently.

A complication arises from the fact that in bulk material the *X* minimum is threefold degenerate. The lattice constant mismatch between GaAs and $Al_xGa_{1-x}As$ produces an anisotropic strain on the $Al_xGa_{1-x}As$ layers: the unit cell is extended along the (001) growth axis and compressed in the perpendicular plane. The strain splits the *X* degeneracy into two distinct bands with very different dispersions as a consequence of the strong anisotropy of the conduction band near the *X* minimum. The upper (lower) band is named X_z (X_{xy}) because the relative effective mass along the growth direction coincides with the bulk effective mass m_z ($m_{x,y}$) along the same (perpendicular) axis; the two masses are indeed very different ($m_z \approx 5.6 m_{xy}$).

Details on the calculations based upon the envelope function approximation are given in the Appendix and Ref. 10. We find that the level X_{xy} is always above X_z in the DBQW's investigated and that, in most cases, X_{xy} is not a confined state in the AlAs layers. For this reason, but also for the sake of simplicity, we discuss the general features of the electronic properties of the DBQW heterostructures referring only to the X_z profile. We will also limit our analysis to DBQW's with ultrathin AlAs layers, namely, only one or two monolayers, such as the heterostructures investigated.

Both the *X* and Γ potential schemes for the DBQW's show the peculiar and interesting feature that bound states are allowed only in a limited range of the GaAs and AlAs layer thicknesses. A similar effect does not exist in standard QW structures, which always admit at least one bound state. Even more interesting is the fact that the *X* and Γ bound levels have a different dependence on the GaAs layer thickness: a Γ (*X*) bound state is present only for relatively thick (thin) GaAs region. In fact, on the one hand, when reducing the width of the GaAs layers one obviously increases the confinement energy of the Γ bound state, which eventually becomes a resonance in the continuum. A Γ bound state can exist only for relatively thick layers of GaAs and this property has been used, for instance, for studying the case of very shallow carrier subbands.[10–14] On the other hand, an *X* bound state is allowed only in very thin GaAs layers; in fact, a large GaAs barrier (see Fig. 1) completely decouples the two AlAs wells, which, being very thin and strongly asymmetric, do not admit any bound state. On the contrary, without the GaAs region the *X* profile corresponds to a standard QW, which, as already noted, always allows at least one bound state. As a matter of fact, the *X* bound level arises from the coupling between the two very thin AlAs wells, which is effective only in the limit of very thin GaAs barriers.

For both the *X* and Γ potential profiles a threshold value $L_{\rm th}^i$ ($i=X,\Gamma$) exists in the GaAs thickness for admitting a bound state. This can be easily calculated, after solving the eigenvalue problem for the Γ (*X*) profile, by imposing the condition that the ground-state energy in Γ (*X*) coincides with the $Al_xGa_{1-x}As$ potential barrier V_B^Γ (V_B^X). The relations obtained between $L_{\rm th}^i$, the AlAs thickness *d*, and the aluminum content *x* (giving the effective masses and the potential barrier height) are

$$L_{\rm th}^\Gamma = \frac{2}{k_w^\Gamma} \arctan[\alpha^\Gamma \tanh(k_b^\Gamma d)], \tag{1}$$

$$L_{\rm th}^X = \frac{2}{k_w^X} \arctan[\alpha^x \tan(k_b^X d)], \tag{2}$$

where

$$\alpha^i = \frac{m_w^i k_b^i}{m_b^i k_w^i}, \quad k_w^i = \sqrt{\frac{2 m_w^i V_B^i}{\hbar^2}}, \quad k_b^i = \sqrt{\frac{2 m_b^i (V_0^i - V_B^i)}{\hbar^2}}$$

for $i=X,\Gamma$ and V_0^i stands for the highest potential barrier, e.g., AlAs in Γ and GaAs in *X*. The numerical values of the parameters depend on the aluminum content *x*, as given in Table I.

Therefore, DBQW's indeed result in a large variety of electronic configurations, as depicted in Fig. 2 in the case of DBQW's with two monolayers (ML's) of AlAs. The dashed (dotted) line in Fig. 2(a) represents the threshold condition for admitting a bound state in the Γ (*X*) potential profile: above (below) this line a bound state exists, while below (above) it, the Γ (*X*) electronic spectrum is a continuum. The continuous line in Fig. 2(a) corresponds to the evolution of the Γ-*X* cross point as a function of the aluminum content when varying the GaAs layer thickness: above it the fundamental electronic level is at the *X* point, while below it the continuous line is at the Γ point. Note also that below five ML's the Γ-*X* cross point tends to the critical value $x_c = 0.38$, which corresponds to the direct-indirect crossover for the alloy. Following these predictions, one can define, therefore, the character of the fundamental electronic level, which can be bound or unbound in both the *X* and the Γ conduction minima.

As a further step one can add the threshold condition for heavy holes just by using Eq. (1) with the corresponding parameters. A sort of phase diagram for the DBQW's can therefore be plotted, such as the one reported in Fig. 2(b). In order to label all the possible configurations we used the standard denomination of type I or type II for describing

TABLE I. Numerical values of the parameters used in the calculations.

Parameter	GaAs	$Al_xGa_{1-x}As$	AlAs
band-gap energy at Γ			
E_g^{Γ} (eV)	1.5194[a]	$1.5194+1.36x+0.22x^2$[b]	3.13[a]
band-gap energy at X			
E_g^{X} (eV)	1.9880[c]	$1.988+0.207x+0.055x^2$[c]	2.25[c]
electron effective mass at Γ			
m_e^{Γ}/m_0	0.0665[d]	$0.0665+0.0835x$[e]	0.15[d]
heavy-hole effective mass			
m_{hh}/m_0	0.3774[f]	$0.3774+0.1011x$[e]	0.4785[f]
light-hole effective mass			
m_{lh}/m_0	0.0904[f]	$0.0904+0.1175x$[e]	0.2079[f]
electron effective mass at X_z			
m^{X_z}/m_0	1.3[a]	$1.3-0.2x$[e]	1.1[a]
electron effective mass at $X_{x,y}$			
$m^{X_{xy}}/m_0$	0.23[a]	$0.23-0.04x$[e]	0.19[a]
elastic stiffness constants			
C_{11} (Mbar)	1.223[g]	$1.223+0.027x$[e]	1.25[g]
C_{12} (Mbar)	0.571[g]	$0.571-0.37x$[e]	0.534[g]
shear deformation potential			
E_2 (eV)	6.5[h]	$6.5-0.07x$[e]	5.8[i]

[a]Reference 19.
[b]Reference 22.
[c]Reference 23.
[d]Reference 24.
[e]Reference 25.
[f]Reference 26.
[g]Reference 20.
[h]Reference 21.
[i]Reference 27.

heterostructures where the electron and hole wave functions are localized mainly in the same or in different spatial regions, respectively. Note that for the peculiarities of the $Al_xGa_{1-x}As$/AlAs/GaAs DBQW's type-I (type-II) character always implies a direct Γ-Γ (indirect Γ-X) fundamental transition in k space. Besides the usual discrimination between type-I and type-II heterostructures, additional features can be stressed concerning the presence, or lack thereof, of a bound state for both the electrons and the holes. We named these different configurations with the first four greek letters as reported in the caption to Fig. 2(b). A very similar phase diagram (the main changes are in the extension of the different regions) is found in the case of DBQW's with one ML of AlAs.

From the phase diagrams of the DBQW heterostructures one obtains that the optimum aluminum percentage for investigating the transition from type-I to type-II recombination is of the order of 40%. In fact, on the one hand, the fundamental electronic level is always at the Γ point of the Brillouin zone below the critical value $x_c=0.38$; on the other hand, it is well known that a high aluminum content produces compositional islands at the alloy surface and therefore results in an increase of the interface roughness and a degradation of the sample quality.

Let us conclude this section with a few remarks on the validity of the envelope function approximation (EFA). The EFA has been shown to be a very simple and powerful theoretical approach for describing the electronic properties of the heterostructures. However, the EFA is, *a priori*, applicable only to relatively thick layers and in the absence of resonances between different points of the Brillouin zone. Both these conditions fail in the case of ultrathin $Al_xGa_{1-x}As$/AlAs/GaAs DBQW's and therefore a more sophisticated theoretical approach is certainly needed for precise quantitative predictions. Nevertheless, it has been found, *a posteriori*, that EFA predictions nicely agree with the experimental findings even outside the *a priori* range of applicability; in particular, both the ultrathin heterostructures and the Γ-X mixing problem have been analyzed recently within this framework. We therefore believe that the EFA can be used as a simple and direct method for qualitatively interpreting the main features in ultrathin $Al_xGa_{1-x}As$/AlAs/GaAs DBQW's without asking for a strict quantitative agreement with the experimental data. In fact, one should also note that in the case of ultrathin DBQW's the numerical predictions of the model critically depend on the choice of the structure parameters (i.e., the effective masses, the band offset, and the $Al_xGa_{1-x}As$ band gap), even if the gross features are always maintained.

III. SAMPLES AND EXPERIMENT

The four samples on which measurements have been made were undoped $Al_xGa_{1-x}As$/AlAs/GaAs DBQW's

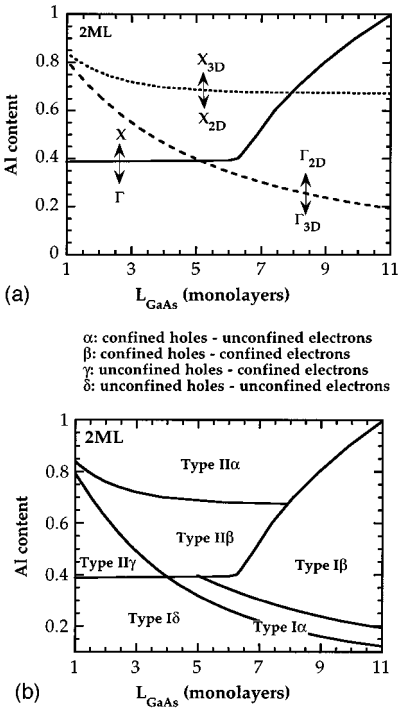

FIG. 2. (a) Electronic configurations in DBQW's with two ML's of AlAs. Full line, evolution of the Γ-X crossover as a function of the Al content when varying the GaAs layer thickness, dashed (dotted) line, threshold condition for admitting a bound state in the Γ (X) potential profile. (b) Recombination types in DBQW's. α, confined holes-unconfined electrons; β, confined holes-confined electrons; γ, unconfined holes-confined electrons; δ, unconfined holes-unconfined electrons.

grown by molecular-beam epitaxy with a nominal aluminum concentration of $x=0.42$; as stressed in the preceding section, $x\approx 0.4$ is indeed the optimum aluminum content for investigating the type-I to type-II transition. The growth parameters were preliminarily determined using reflection high-energy electron diffraction intensity oscillations; the samples were grown on rotating substrates.[11] Each structure contains several DBQW's of different AlAs and GaAs layer thicknesses separated by thick $Al_xGa_{1-x}As$ barriers (300 Å) in order to decouple the carrier wave functions. In the following, the DBQW's will be labeled by the notation (a-b), where a and b stand for the AlAs and GaAs thickness given in monolayers, respectively. Sample 1 contains four DBQW's: (2-9), (2-7), (2-5), and (1-3); sample 2: (1-7), (2-6), and (1-4); sample 3: (1-8), (1-6), and (2-4); and sample 4: (2-8), (1-5), and (1-2). The electronic configuration of these structures is reported in Fig. 2, as resulting from the predictions of the envelope function theory.

Continuous-wave (cw) PL and photoluminescence excitation (PLE) measurements have been performed using a tunable Ar^+ pumped dye laser as the excitation source. The PL signal was dispersed by a 1-m focal length double-grating monochromator and detected by standard lock-in techniques. In the case of time-resolved PL measurements, a synchronously pumped mode-locked dye laser providing pulses with a time duration of the order of 10 ps has been used. The repetition rate has been varied in the range 1–76 MHz by means of a cavity dumper apparatus in order to allow the

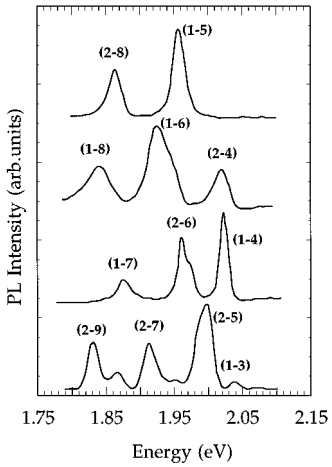

FIG. 3. PL spectra of DBQW's at $T=2$ K after cw excitation. The peaks are labeled according to the AlAs (GaAs) layer thicknesses in ML's.

measurement of decay times up to several hundreds of nanoseconds. The time-resolved detection has been obtained by means of a time-correlated single photon-counting technique with an overall time resolution of about 150 ps. The samples were held in a variable temperature cryostat and the laser intensity was always kept below 10 W/cm^2 in the measurements reported in this work.

IV. RESULTS AND DISCUSSION

A. Continuous-wave measurements

We report in Fig. 3 the PL spectra at $T=2$ K of the DBQW's investigated, together with the assignment of the PL bands. In the case of the (2-9) and (2-7) DBQW's the PL bands clearly show pronounced shoulders on the high-energy side, which are very likely connected to one GaAs monolayer fluctuation, as suggested by their energy position if compared with the PL bands associated with the (2-8) and (2-6) DBQW's. No trace of phonon sidebands are detected in the PL spectra of the different samples. It should be noted also that, for several type-II DBQW's [namely, (1-6), (2-6), and (2-5)], the PL lines are doublets. Possible attributions of the PL doublet are recombination at donor impurities and/or transitions involving the X_z and the $X_{x,y}$ valley; the experimental splitting is, in both cases, in agreement with the theoretical prediction. We are not able to give a definitive attribution, even if the excitation power and temperature dependence of the relative weights suggest that donor impurities[10] play a major role. In any case, a detailed discussion of this point is beyond the scope of this paper.

The most striking feature in the spectra reported in Fig. 3 is certainly the shift of the PL transition energies when both adding AlAs monolayers and reducing the GaAs layer thickness. This is clear evidence of the strong increase of the carrier confinement in the DBQW structures. However, the blueshift of the PL lines associated with the reduction of the GaAs thickness tends to saturate for ultrathin DBQW's, as shown in Fig. 4, where the transition energies are plotted versus the GaAs layer thickness. The change of slope in Fig. 4 can be explained in terms of a type-I–type-II transition of

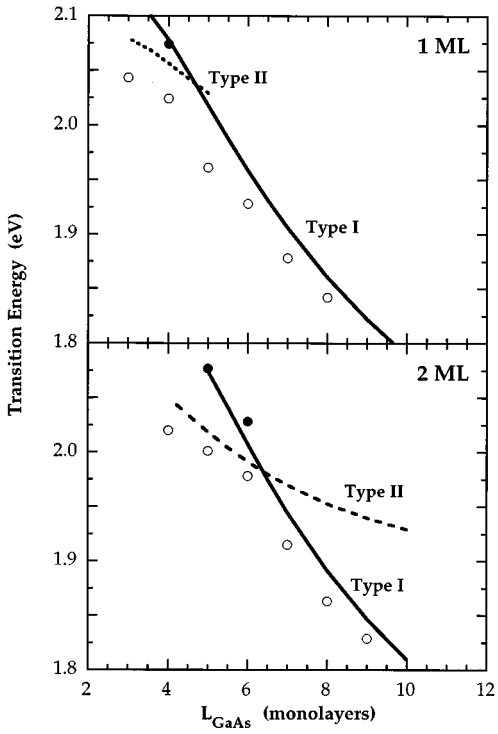

FIG. 4. Transition energies in DBQW's as a function of the GaAs layer thickness. ○ and ●, experimental points; — and - - -, EFA predictions for type-I and type-II structures, respectively.

the DBQW's around the (1-4) and (2-6) heterostructures, as predicted by the effective-mass model and reported in Fig. 2. In fact, in Fig. 4 we also compare the experimental trend with th predicted dependences of the transition energies between the fundamental hole state and the first electron bound level at the Γ (solid line) or at the X (dashed line) profile. Obviously the intersection of the two lines denotes the type-I–type-II crossover and the agreement between the experimental and theoretical trends clearly confirms the change in the type of recombination.

The fact that the direct Γ-Γ and indirect Γ-X transitions have a different dependence on the GaAs thickness arises from the completely different electron potential profiles to which they refer (see Fig. 1). As discussed in Sec. II, the Γ and X electronic states indeed show opposite variations when thinning the GaAs regions: the electron confinement energy increases in the case of the Γ states and decreases in the case of the X levels, respectively. However, the dependence of the recombination energy on the GaAs layer thickness is determined by the energy dependence associated with the lighter carrier and therefore the residual increase of the transition energy in the case of type-II recombination is due to the increase of the heavy-hole confinement energy (the heavy-hole mass is smaller than the X_z electron mass).

Let us now return to the PL spectra reported in Fig. 3. It is worth noting, as a general feature, that most of the supposed type-II transitions show PL intensities comparable to or even higher than those relative to type-I transitions, showing that the nonradiative processes have a similar influence on both kinds of heterostructures. This is rather surprising for a couple of reasons. First, one might expect the nonradiative

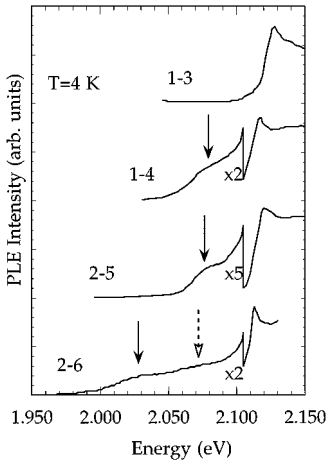

FIG. 5. PLE spectra of type-II DBQW's at $T=4$ K. The arrows mark the fundamental electron–heavy-hole (solid arrow) and electron–light-hole (dotted arrow) transitions at Γ.

processes to be more effective in ultrathin DBQW's due to the larger carrier delocalization in the alloy region, which is well known to be of a poorer quality material compared to GaAs. Second, due to the much longer radiative lifetime in the case of indirect transitions, the radiative efficiency should decrease even for similar nonradiative rates. We therefore conclude that the relevance of the nonradiative mechanisms at low temperatures must be negligible in most of the heterostructures investigated. A different behavior is found in the case of the (1-3) and (1-2) DBQW's. In the first one, the considerable reduction observed in the PL intensity is probably due to a radiative and a nonradiative lifetime of the same order of magnitude, even if a less efficient electron capture can be inferred from the absence of any confined state in the Γ potential profile. Finally, in the case of (1-2) DBQW's, we were not able to detect any PL at all, as expected, due to the fact that heavy holes are not confined anymore (type-II γ DBQW's).

Other interesting information can be derived from the analysis of the PLE spectra, shown in Fig. 5 for type-II structures. On the one hand, they allow us to determine the energy position of the direct excitonic transition in the $Al_xGa_{1-x}As$ barriers, which enables us to estimate the average aluminum content of the alloy in each structure from a comparison with the known x dependence of the $Al_xGa_{1-x}As$ gap as given in Table I. The experimental values give an average aluminum content of about 0.415 (considering all the structures) with an accuracy of about 1–2 %, denoting a high reliability of the design parameters ($x=0.42$). Note also that the experimental value of x has been used for computing the transition energies of each DBQW investigated. On the other hand, on the low-energy side of the PLE spectra we resolve shoulders associated with transitions within the DBQW's. The relative assignments are reported in Fig. 5 and their positions agree nicely with the predictions of the effective-mass model; the estimated Γ-Γ energy transitions for type-II DBQW's are shown by solid circles in Fig. 4. Finally, we were not able to resolve any structure in the case of (1-3) DBQW's, in agreement with the absence of any electron bound states in the Γ potential profile.

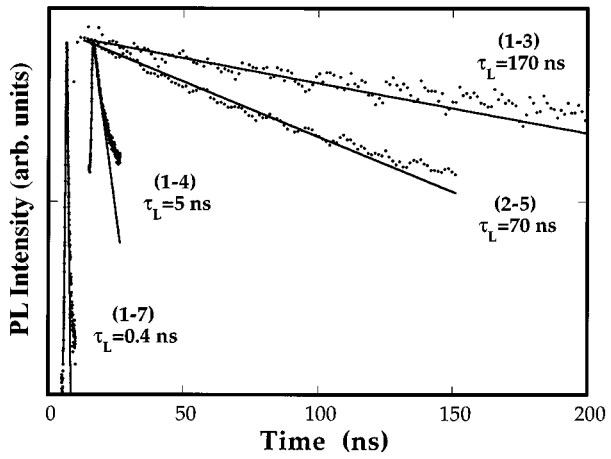

FIG. 6. PL decay in different DBQW's at $T=4$ K after picosecond excitation. The time constants corresponding to the fitting lines are also given.

B. Time-resolved measurements

The transition of the optical recombination from type I to type II in ultrathin DBQW's, predicted by the EFA and confirmed by the cw measurements, is very clearly demonstrated by the time-resolved (TR) measurements reported in Fig. 6. In the case of type-I structures, such as (1-7) and (2-7) DBQW's, we find PL decay times τ_L of the order of 400 ps at 4 K, that is, of the same order of magnitude as the decay times measured in standard GaAs QW's.[12] Reducing the GaAs thickness, τ_L greatly increases: values of the order of 4 ns are found for (2-6) and (1-4) DBQW's, which are near the Γ-X crossover, while much longer values are obtained for type-II structures, namely 70 and 170 ns in the case of (2-5) and (1-3) DBQW's, respectively. This trend is obviously in agreement with the expected increase of the radiative lifetime as soon as the transition switches from direct to indirect (both in k and real space) recombination.

For a more quantitative analysis of the experimental data, one can use the approach proposed by Dawson *et al.*[4] based upon the assumption that the forbidden type-II transitions acquire a nonzero radiative rate as a consequence of Γ-X mixing induced by an effective potential $V_{\Gamma\text{-}X}$. The electronic ground state of type-II structures does not have a pure X character, since it is a mixture of the two nearly resonant Γ and X levels. The radiative lifetime associated with a type-II recombination can then be written as[4]

$$\tau_{\mathrm{II}}=\tau_{\mathrm{I}}\frac{1}{|V_{\Gamma\text{-}X}|^2}\left[\frac{\Delta E_{\Gamma\text{-}X}}{|\langle\Psi_X^e|\Psi_\Gamma^e\rangle|}\right]^2, \tag{3}$$

where $\Delta E_{\Gamma\text{-}X}$ is the energy difference between the Γ and X states, whose wave-function overlap integral appears in the denominator, and τ_{I} is the radiative lifetime of the Γ state $|\Psi_\Gamma^e\rangle$. In order to evaluate τ_{I} for ultrathin DBQW's one has to consider that, due to the Γ-exciton delocalization, it increases when decreasing the GaAs layer thickness. This increase is due essentially to the reduction of the overlap integral between the Γ electron and hole wave functions and a reasonable estimate of τ_{I} is given by[13]

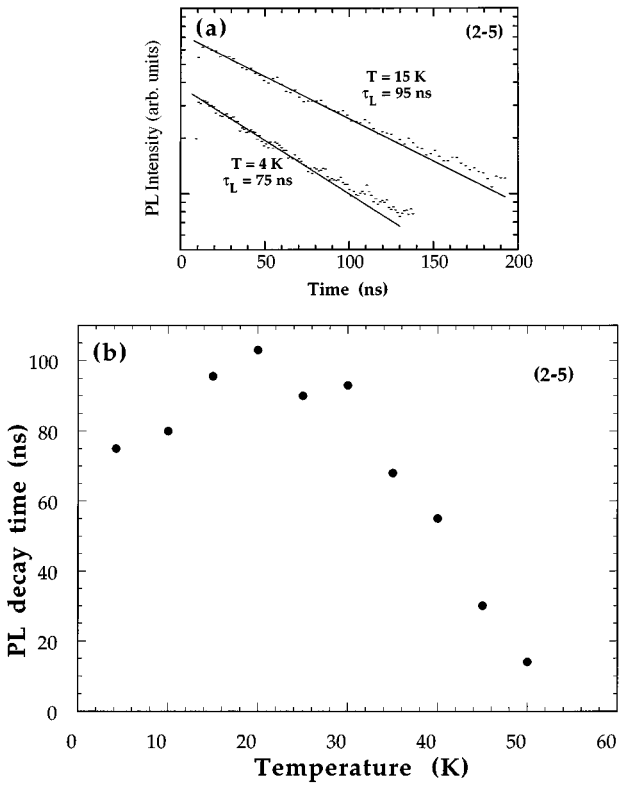

FIG. 7. (a) PL decay of the (2-5) DBQW at two different temperatures. (b) PL decay time versus temperature for the (2-5) DBQW.

$$\tau_{\mathrm{I}}=\frac{\tau_{\mathrm{I0}}}{|\langle\Psi_\Gamma^e|\Psi_\Gamma^{\mathrm{hh}}\rangle|^2}, \tag{4}$$

where τ_{I0} ($\approx$200 ps) is the value corresponding to a standard single quantum well. In the case of the (1-3) DBQW, where the Γ electronic level is not bound, we estimate the overlap integrals in Eqs. (3) and (4) by assuming Ψ_Γ^e to be given by the wave function corresponding to the first resonance in the continuum spectrum (i.e., the energy where the transmission probability is maximum) according to recent results on above-barrier resonances.[14]

Before discussing the predictions of this model for the radiative lifetimes in type-II DBQW's a few remarks are needed. First of all, it should be recalled that τ_L represents the radiative lifetime only if the nonradiative processes are not effective. In fact, as discussed in Sec. IV A, the cw data at low temperatures suggest a very small (if any) contribution from the nonradiative mechanisms, except perhaps in the case of the (1-3) DBQW. The radiative nature of the recombination in our structures is confirmed by the experimental finding, reported in Fig. 7, that the PL decay time τ_L increases with temperature by about 25 ns from 4 to 15 K, as expected for the radiative lifetime.[15] Above 20 K the recombination time starts decreasing, very likely as a consequence of the activation of nonradiative channels and, in particular, of the thermal escape of carriers.[16]

Another point to make is that the time evolution of the PL signal at low T in type-II DBQW's is nonexponential in the time interval investigated, namely, a few hundred nanoseconds after excitation; in fact, at least two time constants are

needed in order to reproduce the experimental data. This feature can be ascribed to the doublet nature of the PL peaks observed in cw measurements, most likely due to the recombination of both free excitons and excitons bound at donor impurities. Due to the large overlap between the two PL bands, the TR measurements, even at the peak energy, contain contributions from both PL lines, which, in principle, are expected to have different decay times. In fact, we find that, increasing the laser intensity, the relative weight of the slower component in the TR spectrum decreases, in agreement with the saturation of the low-energy PL band observed under cw excitation. We therefore assign the slower decay time to the extrinsic recombination of the bound excitons and assume that the faster time is constant (i.e., the decay time at short delays) as representative of the radiative recombination in type-II DBQW's. However, it should be noted that an intrinsic nonexponential behavior of the PL time evolution in type-II structures at low T has been suggested recently.[7]

We find that the experimental recombination times can be fairly accounted for by Eqs. (3) and (4) if the matrix element of the effective mixing potential $|V_{\Gamma\text{-}X}|$ is taken to be of the order of 4 meV. Such a numerical value for the effective mixing potential is in agreement with those estimated in type-II short-period SL's, as reported in Ref. 5. Actually, several mechanisms contribute in determining $V_{\Gamma\text{-}X}$ and most of them are extrinsic in nature, in particular, the interface roughness,[6] which can be very different in different structures. Moreover, DBQW's and SL's are, in many aspects, very different; in the latter a large number of interfaces and a superimposed periodicity along the growth axis are present, while only two interfaces are involved in the case of DBQW's. We believe, therefore, that a comparison between data from DBQW's and SL's is not at all straightforward.

V. CONCLUSION

The insertion of ultrathin layers of AlAs between the $Al_xGa_{1-x}As$ alloy and the GaAs layers provides an important degree of freedom for tailoring the band structure and the optical transition energies of semiconductor heterostructures. As a matter of fact, DBQW's show a large variety of electronic configurations within small changes of the structural parameters; the carrier ground state can be bound or unbound and in the case of the electrons the fundamental level can be both at Γ in GaAs and at X in AlAs. We have demonstrated the transition from type-I to type-II recombination in a set of DBQW's.

Both cw and TR photoluminescence have been used in order to establish the nature of the recombination, but it is probably worth stressing that the two techniques provide very different information. The PL and PLE transition energies measured in a continuous wave essentially reflect the ground-state energies that can be taken into account by simple effective-mass calculations for the separated Γ and X potential profiles. Even if an anticrossing splitting is expected as a consequence of the Γ-X mixing, not only is its value very small in comparison to the carrier confinement energies, but, in addition, it turns out to be of the same order of magnitude as the measured linewidth and the Stokes shift, at least in the samples we have investigated. Moreover, the large inhomogeneous broadening makes it very hard to resolve the weak indirect Γ-X transition in the PLE spectra. Even if Γ-X mixing is the main physical mechanism in determining the excitonic recombination in type-II structures, it is rather difficult to extract information on it from the cw measurements. Completely different is the case of TR PL measurements, since the radiative recombination times are directly determined by the Γ-X mixing. Good agreement is finally obtained between the observed PL decay times and the predictions of a well-known model[4] for the recombination in type-II heterostructures, based on Γ-X mixing effects.

ACKNOWLEDGMENT

The work at LENS has been supported by ECC Contract No. GE1*CT92-0046.

APPENDIX

The electronic levels in the Γ and X profiles have been calculated using the standard transfer matrix formalism of the envelope function approximation.[17] We use the Bastard boundary conditions (e.g., we conserve the envelope wave function and its derivative divided by the effective mass[17]) and the parameters reported in Table I. Nonparabolicity of the Γ conduction band is included self-consistently by considering an energy-dependent effective mass;[18] a conduction band offset of 0.68 has been used.[28] The eigenvalue problem was then solved independently for the Γ and the two X bands. The effect of the lattice mismatch between GaAs and Al(Ga)As has been included following the bulk relationships. Since the DBQW's investigated have been grown on (001) GaAs substrates, the GaAs layers can be considered unstrained and all the strain is found in the AlAs and $Al_xGa_{1-x}As$ layers. The in-plane strain for the AlAs layers is given by[19]

$$e_{\parallel}=e_{xx}=e_{yy}=\frac{a_{\mathrm{GaAs}}-a_{\mathrm{AlAs}}}{a_{\mathrm{AlAs}}}=-1.4\times10^{-3}, \qquad \text{(A1)}$$

while the perpendicular strain is determined by[20]

$$e_{\perp}=e_{zz}=-2\frac{C_{12}}{C_{11}}e_{\parallel}=1.2\times10^{-3}, \qquad \text{(A2)}$$

where the C_{ij} are the AlAs elastic stiffness constants reported in Table I. The $e_{\parallel}$ relative values for the alloy $Al_xGa_{1-x}As$ scale linearly with x following the Vegard law and $e_{\perp}$ can be deduced by means of Eq. (A2). The strain in the AlAs layers induces a hydrostatic shift of all the X states of the order of a few meV.[21] The uniaxial deformation produces a splitting of the X_z and X_x-X_y levels given by[21]

$$\Delta X=E_2(e_{\perp}-e_{\parallel}), \qquad \text{(A3)}$$

where E_2 is the shear deformation potential reported in Table I. This splitting, of the order of 15 meV in the AlAs layers, is divided among the three states according to the relations[20]

$$\Delta X_z=\tfrac{2}{3}\,\Delta X, \quad \Delta X_x=\Delta X_y=-\tfrac{1}{3}\,\Delta X. \qquad \text{(A4)}$$

[1] F. Minami, K. Hirata, K. Era, T. Yao, and Y. Masumoto, Phys. Rev. B **36**, 2875 (1987).
[2] B. A. Wilson, IEEE J. Quantum Electron. **24**, 1763 (1988).
[3] B. A. Wilson, C. E. Bonner, R. C. Spitzer, R. Fisher, P. Dawson, K. J. Moore, C. T. Foxon, and G. W. 't Hooft, Phys. Rev. B **40**, 1825 (1989).
[4] P. Dawson, K. J. Moore, C. T. Foxon, G. W. 't Hooft, and R. P. M. van Hal, J. Appl. Phys. **65**, 3606 (1989).
[5] M. Maaref, F. F. Charfi, D. Scalbert, C. Benoit à la Guillaume, and R. Planel, Phys. Status Solidi B **170**, 637 (1992).
[6] M. Maaref, F. D. Charfi, D. Scalbert, C. Benoit à la Guillaume, R. Planel, and G. Le Roux, Solid State Commun. **84**, 511 (1992).
[7] J. F. Angell and M. D. Sturge, Phys. Rev. B **48**, 4650 (1993).
[8] J. Nunnenkamp, K. Reimann, J. Kuhl, and K. Ploog, Phys. Rev. B **44**, 8129 (1991).
[9] M. Leroux, N. Grandjean, B. Chastaingt, C. Deparis, G. Neu, and J. Massies, Phys. Rev. B **45**, 11 846 (1992).
[10] B. Chastaingt, Doctor thesis, 1993 (unpublished).
[11] G. Neu, Y. Chen, C. Deparis, and J. Massies, Appl. Phys. Lett. **58**, 2111 (1991).
[12] M. Gurioli, A. Vinattieri, M. Colocci, C. Deparis, J. Massies, G. Neu, A. Bosacchi, and S. Franchi, Phys. Rev. B **44**, 3115 (1991).
[13] J. Martinez-Pastor, M. Gurioli, M. Colocci, C. Deparis, B. Chastaingt, and J. Massies, Phys. Rev. B **46**, 2239 (1992).
[14] M. Colocci, J. Martinez-Pastor, and M. Gurioli, Phys. Rev. B **48**, 8089 (1993).
[15] J. Feldmann, G. Peter, E. O. Gobel, P. Dawson, K. Moore, G. Foxon, and R. J. Elliott, Phys. Rev. Lett. **59**, 2337 (1987); **60**, 243 (1988); J. Martinez-Pastor, A. Vinattieri, L. Carraresi, M. Colocci, Ph. Roussignol, and G. Weimann, Phys. Rev. B **47**, 10 456 (1993).
[16] M. Gurioli, J. Martinez-Pastor, M. Colocci, C. Deparis, B. Chastaingt, and J. Massies, Phys. Rev. B **46**, 6922 (1992).
[17] G. Bastard, *Wave Mechanics Applied to Semiconductor Heterostructures* (Les editions de Physique, Les Ulis Cedex, 1988).
[18] D. F. Nelson, R. C. Miller, and D. A. Kleinman, Phys. Rev. B **35**, 7770 (1987).
[19] S. Adachi, J. Appl. Phys. **58**, R1 (1985).
[20] G. Chris and L. Van de Valle, Phys. Rev. B **39**, 1871 (1989).
[21] H. W. van Kesteren, E. C. Cosman, P. Dawson, K. J. Moore, and C. T. Foxon, Phys. Rev. B **39**, 13 426 (1989).
[22] C. Bosio, J. L. Staelhi, M. Guzzi, G. Burri, and R. A. Logan, Phys. Rev. B **38**, 3263 (1988).
[23] M. Guzzi, E. Grilli, S. Oggioni, J. L. Staelhi, C. Bosio, and L. Pavesi, Phys. Rev. B **45**, 10 951 (1992).
[24] *Numerical Data and Functional Relationships in Science and Technology*, edited by O. Madelung, M. Shultz, and H. Weiss (Springer-Verlag, Berlin, 1982).
[25] We assume a linear interpolation between the reported values for GaAs and AlAs.
[26] J. M. Luttinger, Phys. Rev. **102**, 1030 (1955).
[27] S. Charbonneau, J. F. Young, and P. T. Coleridge, Phys. Rev. B **44**, 8312 (1991).
[28] D. J. Wolford, T. F. Kuech, J. A. Bradley, M. A. Gell, D. Ninno, and M. Jaros, J. Vac. Sci. Technol. B **4**, 1043 (1986).